Table VI
Slope and Intercept Obtained from Plots of Eq 7

	intercept	slope	$(1 - r)$	$(D_{Na^+}/D_{Na^+}^\circ)_{min}$
NaPA	−0.15 ± 0.09	0.62 ± 0.03	0.38 ± 0.02	0.38
NaPSC	−0.14 ± 0.09	0.58 ± 0.03	0.42 ± 0.02	0.45
NaPVS	−0.05 ± 0.04	0.38 ± 0.03	0.62 ± 0.05	0.63
NaPSS	−0.03 ± 0.03	0.39 ± 0.02	0.61 ± 0.03	0.62

4, listed in Table VI, are close to the origin within experimental error and the slopes are 0.62 ± 0.03 for NaPA, 0.58 ± 0.03 for NaPSC, 0.38 ± 0.03 for NaPVS, and 0.39 ± 0.02 for NaPSS. For carboxylate polyelectrolytes, the resulting charge fractions $(1 - r)$ of 0.38 and 0.42 for NaPA and NaPSC, respectively, compare excellently with the theoretical values of ξ^{-1} for these polyelectrolytes. This gives some validity to calculate a charge fraction from eq 7, which states that condensation is the dominant interaction. For the sulfonate polyelectrolytes, however, the calculated charge fractions of 0.62 and 0.61, for NaPVS and NaPSS, respectively, deviate from the predicted theoretical value of ξ^{-1}. It appears that the fraction of condensed or bound Na^+ ions originally on the polyelectrolyte, and therefore the polyelectrolyte charge fraction, depends on the nature of the charge groups on the polyion.

It is interesting that the additivity rule (eq 6) and the charge fraction equation (eq 7) are of the same form, with $(D_{Na^+}/D_{Na^+}^\circ)_p$ identified with $(1 - r)$. When plotted as $(D_{Na^+}/D_{Na^+}^\circ)_X(1 + X)$ vs. X, both eq 6 and 7 gave straight lines for $\xi > 1$, with the phenomenological parameters $(D_{Na^+}/D_{Na^+}^\circ)_p$ and $(1 - r)$ independent of N_s. Both phenomenological parameters are close in value for each polyelectrolyte studied here. Equations 6 and 7 stem from the same concept that Na^+ ions are either condensed onto the polyion and do not contribute to the measured D_{Na^+} or that the Na^+ ions are free so as to *not* interact with the polyion and contribute to the measured D_{Na^+}. The interpretation of Wall[20] for $(D_{Na^+}/D_{Na^+}^\circ)_p$ as the degree of dissociation of the polyelectrolyte is consistent with the values obtained for $(1 - r)$ from eq 7. The theoretical equation of Manning, eq 4, can be cast in the same form as eq 6 and 7 if the Debye–Hückel interaction term vanishes. Then, the theoretical value for the fraction of Na^+ ions dissociated from the polyion ξ^{-1} is identified with $(D_{Na^+}/D_{Na^+}^\circ)_p$ of eq 6 and $(1 - r)$ of eq 7. It becomes clearer then as to why eq 6 and 7 should appear to be valid. For high charge density polyelectrolytes, i.e., those used in the present study, the contribution of the condensation term to $D_{Na^+}/D_{Na^+}^\circ$ in eq 4 is much greater than that of the interaction term A.

Registry No. Na^+, 17341-25-2; sodium polyacrylate (homopolymer), 9003-04-7; sodium poly(*p*-styrenecarboxylate) (homopolymer), 92078-72-3; poly(sodiumvinylsulfonate) (homopolymer), 9002-97-5; sodium poly(styrenesulfonate) homopolymer, 9080-79-9.

References and Notes

(1) Ander, P.; Kardan, M. *Macromolecules* **1984**, *17*, 2431.
(2) Kowblansky, M.; Zema, P. *Macromolecules* **1981**, *14*, 1448.
(3) Manning, G. S. *J. Chem. Phys.* **1969**, *51*, 924.
(4) Manning, G. S. *J. Chem. Phys.* **1969**, *51*, 934.
(5) Manning, G. S. *J. Chem. Phys.* **1969**, *51*, 3249.
(6) Manning, G. S. *Biophys. Chem.* **1977**, *7*, 95.
(7) Manning, G. S. *Annu. Rev. Phys. Chem.* **1972**, *23*, 117.
(8) Manning, G. S. *Q. Rev. Biophys.* **1978**, *11*, 179.
(9) Manning, G. S. *Acc. Chem. Res.* **1979**, *12*, 443.
(10) Leebrick, J. R.; Ramsden, H. E. *J. Org. Chem.* **1958**, *23*, 935.
(11) Mandelkern, L.; Flory, P. J. *J. Chem. Phys.* **1952**, *20*, 212.
(12) Eisenberg, H.; Woodside, D. *J. Chem. Phys.* **1962**, *36*, 1844.
(13) Noda, I.; Tsuge, T.; Nagasawa, M. *J. Phys. Chem.* **1970**, *74*, 710.
(14) Takahashi, A.; Kato, T.; Nagasawa, M. *J. Phys. Chem.* **1967**, *71*, 2001.
(15) Anderson, J. S.; Saddington, K. *J. Chem. Soc.* **1949**, S381.
(16) Prini, R.; Lagos, A. *J. Polym. Sci., Part A* **1964**, *2A*, 2917.
(17) Ander, P.; Gangi, G.; Kowblansky, A. *Macromolecules* **1978**, *11*, 904.
(18) Lubas, W.; Ander, P. *Macromolecules* **1980**, *13*, 318.
(19) Savner, S. Senior Thesis, Seton Hall University, 1982.
(20) Huizenga, J. R.; Grieger, P. F.; Wall, F. T. *J. Am. Chem. Soc.* **1950**, *72*, 4228.
(21) Oman, S.; Dolar, D. *Z. Phys. Chem. (Wiesbaden)* **1967**, *56*, 1.
(22) Ander, P.; Lubas, W. *Macromolecules* **1981**, *14*, 1058.
(23) Begala, A. J.; Strauss, U. P. *J. Phys. Chem.* **1972**, *76*, 254.
(24) Yoshida, N. *J. Chem. Phys.* **1978**, *69*, 4867.
(25) Strauss, U. P.; Leung, Y. P. *J. Am. Chem. Soc.* **1965**, *87*, 1476.
(26) Matti, J.; Kwak, C. T. *J. Phys. Chem.* **1982**, *86*, 1026.
(27) Tondre, C.; Zana, R. *J. Phys. Chem.* **1971**, *75*, 21.
(28) Eldridge, R. J.; Treloar, F. E. *J. Phys. Chem.* **1970**, *74*, 1446.
(29) Podlas, T. J.; Ander, P. *Macromolecules* **1970**, *3*, 154.
(30) Trifiletti, R.; Ander, P. *Macromolecules* **1979**, *12*, 1197.
(31) Kowblansky, M.; Ander, P. *J. Phys. Chem.* **1976**, *80*, 297.
(32) Kowblansky, M.; Tomasula, M.; Ander, P. *J. Phys. Chem.* **1978**, *82*, 1491.
(33) Kowblansky, M.; Zema, P. *Macromolecules* **1981**, *14*, 166.
(34) Ander, P. In "Solution Properties of Polysaccharides"; Brant, D., Ed.; American Chemical Society: Washington, DC, 1981; ACS Symp. Ser. No. 150, Chapter 28.
(35) Anderson, C.; Record, M.; Hart, P. *Biophys. Chem.* **1978**, *7*, 301.

Notes

Monte Carlo Calculation of the Friction Coefficient and Viscosity Number of Wormlike Star Molecules. 2

BRUNO H. ZIMM

Department of Chemistry, B-017, University of California (San Diego), La Jolla, California 92093.

Received January 18, 1984

In a recent article[1] we reported preliminary results from Monte Carlo calculations of the effects of star branching on the sedimentation and viscosity of dilute solutions of polymers. Here we extend these calculations to larger model molecules and larger ensembles with smaller statistical errors. We have also included an ensemble with excluded volume, corresponding to solutions in good solvents. In general, the new results confirm the trends seen in the earlier ones; most notably, the viscosity ratio, g', is consistently less than the ratio of root-mean-square radii, $g^{1/2}$.

The calculations were carried out on ensembles of rigid-body chain models, both with and without preaveraging of the hydrodynamic interactions. The calculations on models without excluded volume were carried out as before, except that 100 chains each of 49 beads were generated in each case instead of 50 chains of 25 beads. Each such run consumed about 40 min of processor time on the VAX 11-780. In addition, we generated models in which all approaches of beads closer than twice the hydrodynamic

0024-9297/84/2217-2441$01.50/0

Table I
With No Excluded Volume

	$a' = 0$			$a' = 0.84$		
f	2	4	6	2	4	6
R^2	8.77 ± 0.6	5.2 ± 0.2	3.92 ± 0.1	19.1 ± 1.1	12.3 ± 0.6	8.03 ± 0.2
u	1.17 ± 0.02	1.24 ± 0.01	1.31 ± 0.01	0.942 ± 0.01	0.979 ± 0.01	1.06 ± 0.01
u,kr	1.33 ± 0.02	1.45 ± 0.02	1.59 ± 0.02	1.05 ± 0.01	1.14 ± 0.01	1.25 ± 0.01
u/u,kr	0.880 ± 0.006	0.854 ± 0.005	0.824 ± 0.005	0.895 ± 0.004	0.860 ± 0.006	0.848 ± 0.005
E	6.24 ± 0.4	4.45 ± 0.2	3.62 ± 0.1	13.9 ± 0.8	10.4 ± 0.5	7.50 ± 0.3
E,kr	7.13 ± 0.4	5.53 ± 0.2	4.85 ± 0.1	14.9 ± 0.8	11.5 ± 0.5	8.83 ± 0.3
E/E,kr	0.875 ± 0.01	0.804 ± 0.01	0.746 ± 0.01	0.930 ± 0.01	0.909 ± 0.01	0.849 ± 0.02
$g^{1/2}$	1	0.770 ± 0.030	0.669 ± 0.025	1	0.802 ± 0.031	0.648 ± 0.021
h	1	0.948 ± 0.018	0.895 ± 0.017	1	0.962 ± 0.014	0.892 ± 0.013
h,kr	1	0.921 ± 0.019	0.837 ± 0.016	1	0.925 ± 0.012	0.845 ± 0.011
h/h,kr	1	1.03 ± 0.009	1.07 ± 0.010	1	1.04 ± 0.009	1.06 ± 0.008
g'	1	0.713 ± 0.056	0.580 ± 0.041	1	0.752 ± 0.056	0.540 ± 0.038
g',kr	1	0.776 ± 0.052	0.681 ± 0.041	1	0.769 ± 0.053	0.591 ± 0.037
g'/g',kr	1	0.919 ± 0.016	0.852 ± 0.015	1	0.977 ± 0.015	0.913 ± 0.024

Table II
With Excluded Volume

	$a' = 0$			$a' = 0.84$		
f	2	4	6	2	4	6
atten[a]		87.8	909	14.5	24.3	59.9
R^2	15.7 ± 0.6	9.87 ± 0.3	7.08 ± 0.2	33.3 ± 1.4	20.3 ± 0.6	13.3 ± 0.3
u	0.928 ± 0.009	0.992 ± 0.008	1.05 ± 0.007	0.758 ± 0.008	0.806 ± 0.007	0.868 ± 0.007
u,kr	0.996 ± 0.01	1.10 ± 0.01	1.18 ± 0.008	0.803 ± 0.01	0.88 ± 0.009	0.965 ± 0.008
u/u,kr	0.932 ± 0.002	0.903 ± 0.002	0.888 ± 0.003	0.944 ± 0.002	0.916 ± 0.003	0.899 ± 0.003
E	12.2 ± 0.4	8.93 ± 0.3	6.85 ± 0.1	26.7 ± 1.1	18.9 ± 0.5	13.4 ± 0.3
E,kr	12.8 ± 0.4	9.98 ± 0.3	8.22 ± 0.2	27.5 ± 1.1	20.2 ± 0.5	15.1 ± 0.3
E/E,kr	0.952 ± 0.007	0.895 ± 0.006	0.833 ± 0.006	0.974 ± 0.006	0.937 ± 0.005	0.886 ± 0.007
$g^{1/2}$	1	0.793 ± 0.020	0.672 ± 0.016	1	0.782 ± 0.020	0.633 ± 0.015
h	1	0.935 ± 0.012	0.887 ± 0.010	1	0.940 ± 0.013	0.873 ± 0.012
h,kr	1	0.906 ± 0.012	0.846 ± 0.010	1	0.913 ± 0.015	0.832 ± 0.012
h/h,kr	1	1.03 ± 0.003	1.05 ± 0.004	1	1.03 ± 0.004	1.05 ± 0.004
g'	1	0.734 ± 0.034	0.563 ± 0.020	1	0.707 ± 0.035	0.500 ± 0.023
g',kr	1	0.780 ± 0.034	0.643 ± 0.025	1	0.734 ± 0.035	0.549 ± 0.025
g'/g',kr	1	0.940 ± 0.009	0.876 ± 0.009	1	0.962 ± 0.008	0.910 ± 0.009

[a] Attenuation factor: ratio of number of chains attempted to number that survived excluded-volume test.

diameter of 0.27135 (in units of the root-mean-square bond length) were eliminated by deleting such chains from the ensemble; the surviving chains were expected to simulate real chains in good solvents. The distribution function that created the bonds was the same Gaussian that was used before. Again, 100 surviving chains of 49 beads were generated in each case. The value 0.84 was chosen for the persistence length, a', to maintain the ratio a'/R the same as before although the values of each were greater. Results are shown in Tables I and II.

The notation is the same as before: f is the number of arms, u and E are dimensionless numbers proportional to the sedimentation coefficient and viscosity number, respectively, R^2 is the mean-square radius, h is the ratio of sedimentation rates of the linear to the branched chains, and g and g' are the ratios of the mean-square radii and the viscosities of the branched to the linear chains. The digraph kr again indicates use of the preaveraged Kirkwood–Riseman hydrodynamic interaction tensor.

Learning from our experience with the previous calculation, we calculated the ratio of the preaveraged and nonpreaveraged sedimentation rates and of the corresponding viscosity numbers for each chain generated and then calculated the standard deviation of these ratios in each ensemble. These provided estimates of the precision of the ratios of the ensemble averages of the preaveraged to nonpreaveraged sedimentation rates and viscosities, statistics that were lacking in the previous work. (The ensemble averages of the ratios were not, of course, exactly equal to the ratios of the ensemble averages, but we presume that the precision measures of the former are good estimates of the precision measures of the latter.) These precision measures were then extended to the corresponding h and g' ratios by standard propagation-of-error methods. The other precision measures were obtained as before.

Discussion

In a valuable recent paper, Fixman[2] has shown that the true sedimentation rate must lie between the nonpreaveraged rigid-body calculations and the preaveraged ones. He also showed that the nonpreaveraged rigid-body viscosity number is an upper bound on the true value, but no corresponding statement can be made about the preaveraged viscosity number (we quoted this conclusion incorrectly in the previous paper[1]). In view of these limits and noting that the nonpreaveraged and preaveraged sedimentation ratios h are close to each other, we can fairly conclude from our results that the sedimentation rate is not nearly as sensitive to branching as the radius ratio, $g^{1/2}$. This is in accord with experiments, as summarized by Roovers et al.[4,5]

Conversely, the nonpreaveraged viscosity ratio, g', is more sensitive to branching than either g',kr or $g^{1/2}$. The nonpreaveraged viscosity numbers, E, are upper bounds to the true values, and since they are lower than the preaveraged ones, E,kr, they must be closer to the true values than the latter; thus g' should be more reliable than g',kr. The ratio of g'/g',kr has better precision than either of its components; this ratio shows that g',kr consistently underestimates the effect of branching in comparison to g'. This increased sensitivity of g' to branching is in better

accord with the experiments.[3-5]

These results reinforce the conclusion of the previous paper[1] that much of the deviation of experiments on star molecules from the predictions based on preaveraging[6,7] can be attributed to the latter approximation. We would like to note, however, that the deviations are modest, and preaveraging remains a useful tool for approximate calculations because of its relative simplicity.

There seems to be no clear effect of either persistence or excluded volume on g'; such differences as appear are within the precision measures. Thus we would not expect solvent power to have much effect on h and g'. In the experiments a small decrease in g' was observed in going from Θ to good solvents.[4,5] For example, the nonpreaveraged g' values for six-armed stars with no persistence are 0.58 ± 0.04 and 0.56 ± 0.03, respectively, without and with excluded volume; Roovers and Bywater's[4] corresponding experimental ones were 0.63 and 0.57. One would naively expect that excluded volume would cause branched molecules to expand more than linear ones, and hence push g and g' nearer unity, and clearly a decided expansion effect does occur, as the figures in the tables show. However, the distribution of sizes is also narrowed, as the standard deviations in the tables also show, and the character of the distribution is probably changed. These changes in distribution apparently overcome the simple effect of expansion on g'.

Acknowledgment. This work was supported by Grant GM-11916 from the National Institutes of Health.

References and Notes

(1) Zimm, B. H. *Macromolecules* **1984**, *17*, 795.
(2) Fixman, M. *J. Chem. Phys.* **1983**, *78*, 1588.
(3) Berry, G. C. *J. Polym. Sci., Part A-2* **1971**, *9*, 687.
(4) Roovers, J. E. L.; Bywater, S. *Macromolecules* **1972**, *5*, 384; **1974**, *7*, 443.
(5) Roovers, J. E. L.; Hadjichristidis, N.; Fetters, L. J. *Macromolecules* **1983**, *16*, 214.
(6) Stockmayer, W. H.; Fixman, M. *Ann. N.Y. Acad. Sci.* **1953**, *57*, 334.
(7) Zimm, B. H.; Kilb, R. W. *J. Polym. Sci.* **1959**, *37*, 19.

Carob Gum–κ-Carrageenan Mixed Gels: Mechanical Properties and X-ray Fiber Diffraction Studies

MERVYN J. MILES,* VICTOR J. MORRIS, and VINCENT CARROLL

AFRC Food Research Institute, Colney Lane, Norwich, NR4 7UA, U.K. *Received October 21, 1983*

The solution properties of certain polysaccharides may be drastically modified by the addition of certain galactomannans.[1,2] Such additions may lead to an enhancement of the viscosity of the mixed-polymer solution, gelation may occur under conditions for which neither pure polymer would gel, or the mechanical properties and texture of the mixed gel may differ from those of either pure polymer gel.

Synergistic polymer–polymer interactions are attractive commercially and enjoy widespread technological exploitation.[3] Expensive polysaccharides may be replaced by cheaper polysaccharides, leading to savings in cost. Mixtures offer the potential for creating new textures or manipulating the rheology and texture. Synergistic polymer–polymer interactions are believed to mimic natural associations of polymers in complex cellular structures,[4] and certain interactions between the extracellular microbial polysaccharide xanthan and plant glycans have been implicated in biological host–pathogen recognition processes.[5]

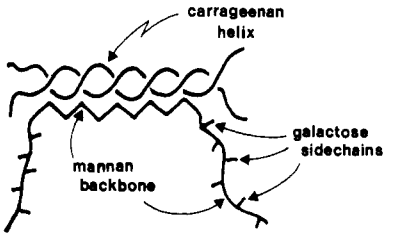

Figure 1. Proposed model[1,2,4] for the interaction between carob gum and κ-carrageenan. Regions of mannan backbone, unsubstituted with galactose side chains, are pictured binding to a carrageenan double helix.

κ-Carrageenan–carob (locust bean) gum mixtures provide a convenient model for studying synergistic interactions. κ-Carrageenan forms brittle transparent thermoreversible gels. Addition of carob gum leads to gelation at total polymer concentrations less than that at which the carrageenan alone will gel.[2] The mixed gels are soft and tough and will sustain substantial tensile plastic deformation.[2] The presently accepted model for gelation is commonly illustrated[1,2,4] as shown in Figure 1 although the stoichiometry and the total number of polymer molecules contributing to a junction zone are vague and unspecified.

The idealized repeat unit[6] for κ-carrageenan (α(1→3)-galactose 4-sulfate–β(1→4)-3,6-anhydrogalactose) is capable of forming threefold right-handed helices.[7,8] Structural regularity is marred by the presence[9] of "kinks" which are believed to restrict helix formation to short segments[10] within the polymer chain. Gelation is claimed to involve an intertwining of two separate chains to form a double-helical region limited by kinking residues, followed by a cation-mediated association of these helices into aggregated or microcrystalline junction zones.[11] At present there is some debate as to whether the helix formation involves an "intermolecular" or "intramolecular" process.[11,12] The binding region of the carrageenan in mixed gels is claimed to be a double-helical segment.[1,2] Carob gum is a galactomannan with a structure based on a β-D-(1→4)-mannan backbone solubilized by substitution with α-D-(1→6)-linked galactose side chains.[2] For carob gum the mannose:galactose (MG) ratio is 3.55, although preparations are likely to be heterogeneous with respect to MG and side-chain distribution.[2] Gelation may occur on standing or be induced by freeze–thaw cycling or the addition of solutes believed to reduce water activity in carob gum solutions.[1,2] Gelation is favored by a high MG, and natural association is believed to occur via unsubstituted regions of the mannan backbone.[1,2] In mixed gels such unsubstituted mannose regions are believed to bind the carrageenan helix[1,2] (Figure 1).

The interactions between polysaccharides and galactomannans are sensitive to the choice of galactomannan and of polysaccharide.[1,2] Carob gum interacts strongly with agar, carrageenan, or xanthan whereas guar gum (MG = 1.63) shows weak interactions.[1,2] Initial X-ray diffraction,[13] chemical,[14] and enzymatic[15] studies implied a uniform distribution of galactose on every second mannose for guar but a block structure for carob gum. Selectivity with respect to galactomannan was attributed to galactose distribution rather than content.[1,2] Recent studies using enzyme,[16] chemical,[17] NMR[18] and X-ray diffraction[19] methods suggest an irregular to random galactose distribution for both guar and carob gum. The suggested model (Figure 1) may still account for selectivity of galactomannan because the higher MG value for carob gum would favor more or longer bare mannan regions. However, the

0024-9297/84/2217-2443$01.50/0